Published in final edited form as:
J Immunol. 2013 March 1; 190(5): 2017–2026. doi:10.4049/jimmunol.1201292.

Spatial coupling of JNK activation to the B cell antigen receptor by tyrosine-phosphorylated ezrin1

Neetha Parameswaran, **Gospel Enyindah-Asonye**, **Nayer Bagheri**[2], **Neilay B. Shah**[3], and **Neetu Gupta**[4]
Department of Immunology, Lerner Research Institute, Cleveland Clinic, 9500 Euclid Avenue, NE40, Cleveland, OH 44195

Abstract

The Ezrin-Radixin-Moesin (ERM) proteins regulate B lymphocyte activation via their effect on BCR diffusion and microclustering. This relies on their ability to dynamically tether the plasma membrane with actin filaments that is in turn facilitated by phosphorylation of the conserved threonine residue in the actin-binding domain. Here, we describe a novel function of ezrin in regulating JNK activation that is mediated by phosphorylation of a tyrosine (Y353) residue that is unconserved with moesin and radixin. BCR, but not CD40, TLR4 or CXCR5 stimulation, induced phosphorylation of ezrin at Y353 in mouse splenic B cells. Ezrin existed in a preformed complex with Syk in unstimulated B cells and underwent Syk-dependent phosphorylation upon anti-IgM stimulation. Y353-phosphorylated ezrin co-localized with the BCR within minutes of stimulation and co-trafficked with the endocytosed BCRs through the early and late endosomes. The T567 residue of ezrin was rephosphorylated in late endosomes and at the plasma membrane at later times of BCR stimulation. Expression of a non-phosphorylatable Y353F mutant of ezrin specifically impaired JNK activation. BCR crosslinking induced the association of Y353-phosphorylated ezrin with JNK and its kinase MKK7, and spatial co-localization with phosphorylated JNK in the endosomes. The YFP-tagged Y353F mutant displayed reduced co-localization with the endocytosed BCR as compared to wild type Ezrin-YFP. Taken together, our data identify a novel role for ezrin as a spatial adaptor that couples JNK signaling components to the BCR signalosome, thus facilitating JNK activation.

INTRODUCTION

Antigen recognition by the BCR in mature B cells triggers a signaling cascade that culminates in transcriptional activation and proliferation (1, 2). At the outset, BCR signaling is accompanied by actin cytoskeletal reorganization that facilitates the formation of BCR microclusters, antigen gathering by the spreading B cell, and the assembly of BCR signalosomes (3, 4). This coordination between intracellular signaling molecules and the cytoskeleton modulates the strength of B cell activation (3, 5, 6). Clustering of the BCR signalosomes is also accompanied by rapid internalization and trafficking of the antigen-bound BCRs to the late endosomes for further processing of the antigen and loading on MHC II molecules (7). The endocytosed BCRs in turn co-segregate with tyrosine and serine/threonine kinases within the endosomal compartments and continue to support signal

[1]This work was supported by an NIH grant from the National Institute of Allergy and Infectious Diseases (AI081743), and an Investigator Award from the Cancer Research Institute to N.G.

[4]Corresponding author: Neetu Gupta, Ph.D., Department of Immunology, Lerner Research Institute, Cleveland Clinic, 9500 Euclid Avenue, NE40, Cleveland, OH 44195 Phone: (216) 444-7455, Fax: (216) 444-9329, guptan@ccf.org.
[2]Current address: Department of Pathology, Case Western Reserve University, 10900 Euclid Avenue, Cleveland, OH 44106
[3]Current address: Haverford College, 370 Lancaster Ave, Haverford, PA, 19041

transduction (8). It is very likely that cytoskeleton-regulating proteins influence the assembly of intracellular signaling components with the BCR in endosomal signalosomes and play an important role in regulating BCR signaling.

The cortical actin filaments are held underneath the plasma membrane by adaptor proteins that tether transmembrane proteins to actin. Ezrin, a plasma membrane-actin cytoskeleton crosslinking protein of the ERM family, contains a conserved threonine residue (T567) in its C-terminal actin-binding domain. Phosphorylation of this threonine is critical for conformational activation and plasma membrane-cytoskeleton crosslinking activity of ERM proteins (9). We previously reported that ezrin is constitutively phosphorylated at T567 in naïve B cells, and dephosphorylation of this site upon BCR stimulation results in conformational inactivation facilitating lipid raft coalescence (10). Similarly, chemokine exposure induces T567 dephosphorylation in ezrin in B cells and the resulting uncoupling of plasma membrane from the actin cytoskeleton is required for the morphological and cytoskeletal changes essential for B cell migration (11). Ezrin-rich networks confine BCR mobility in the absence of antigen (5), but undergo dynamic remodeling upon antigen stimulation to facilitate antigen-receptor clustering (12). Therefore, antigen-induced conformational inactivation of ezrin is an important regulator of membrane dynamics during BCR signal transduction.

High structural homology between ezrin and moesin and their well established role as membrane-cytoskeletal crosslinkers has led to the notion that the two proteins have redundant function in lymphocyte activation and migration (9). Indeed, ezrin-deficient mature T cells show defect in TCR-dependent IL-2 production, which is exacerbated upon additional knock down of moesin expression (13). Interestingly, despite high overall homology between ezrin and moesin, the amino acid sequence of ezrin contains unique phosphorylation sites (S66, Y353 and Y477), and a poly-proline stretch at 469–475 (14), suggesting that ezrin may have additional unconserved context-dependent roles. These features in ezrin may enable protein-protein interactions to facilitate signal transduction and/or localization of interacting proteins. S66-phosphorylated ezrin regulates trafficking of H^+, K^+-ATPase to the apical membrane of gastric parietal cells and is essential for histamine-induced acid secretion (15). Growth factor-dependent phosphorylation of ezrin at Y353 was shown to regulate survival of non-hematopoietic cells (16, 17), whereas Y477 phosphorylation of ezrin regulates growth and invasion of Src-transformed epithelial cells in a three-dimensional environment (18). In human B lymphoma cells, CD81 crosslinking was shown to induce Y353 phosphorylation of ezrin that recruits F-actin and facilitates cytoskeletal reorganization (19). Whether any of these alternate phosphorylation sites contribute towards BCR signaling has not been explored.

In this study we report that BCR crosslinking induces phosphorylation of Syk-associated ezrin at Y353. Y353-phosphorylated ezrin associates with MKK7 and JNK, and couples proximal BCR signaling with the JNK activation machinery in the endosomes, highlighting a novel role for ezrin as a spatial adaptor in the JNK activation pathway.

MATERIALS AND METHODS

Mice and cells

C57BL/6 (B6) mice were bred in our animal colony, and $Lyn^{-/-}$ mice were obtained from Dr. Anthony DeFranco (UCSF). Mice were used at 8–12 weeks of age and all experiments were approved by the Institutional Animal Care and Use Committee of the Cleveland Clinic. The murine B lymphoma cell line CH27 was cultured in DMEM medium supplemented with 15% FBS. The DT40 chicken B cell lines were maintained in DMEM supplemented with 10% FBS and 5% chicken serum. Btk-deficient DT40 cell line was obtained from Dr.

Arthur Weiss (UCSF). Primary B cells were purified from spleens of B6 and Lyn$^{-/-}$ mice using CD43 microbeads (Miltenyi Biotec).

Plasmids and transfection

The Ezrin-pIRES2-eGFP and Ezrin-YFP constructs have been previously described (11), and were used to mutate the tyrosine 353 residue to phenylalanine resulting in the Y353F and Y353F-YFP constructs, respectively. Mutagenesis was performed using the QuickChange® II Site-Directed mutagenesis kit (Stratagene). CH27 cells were transfected with 3–6 μg of the appropriate plasmids using Amaxa Nucleofector II (Lonza).

Cell lysis, immunoblotting and immunoprecipitation

CH27 cells were transfected with vector alone, Y353F, Ezrin-YFP or Y353F-YFP and stimulated with 10 μg/ml of anti-IgM at 37 °C for the indicated times. Lysates were prepared as previously described (11) and resolved by SDS-PAGE followed by immunoblotting with appropriate primary and secondary antibodies. In some experiments, purified splenic B cells were pretreated with 50 μM of PP1 (Calbiochem) or indicated concentrations of piceatannol (Calbiochem) for 30 min at 37 °C prior to stimulation with anti-IgM. For immunoprecipitation, CH27 cell lysates were incubated with appropriate antibodies and protein G-agarose beads (Invitrogen). Alternatively, lysates were incubated with GST-c-Jun fusion protein-conjugated Sepharose beads (Cell Signaling Technology) to precipitate JNK. Immunoblots were subjected to densitometric analysis using ImageJ software for quantification of ratios.

Flow cytometry assays

Surface IgM expression on the vector and Y353F transfectants of CH27 cells was compared by immunostaining with anti-IgM-APC (BD Biosciences) for 30 min at 37 °C. For BCR internalization assay vector and Y353F transfectants of CH27 cells were stained with biotin-conjugated anti-IgM for 30 min on ice, stimulated at 37 °C for the indicated times, fixed and stained with streptavidin-conjugated phycoerythrin (BD Biosciences) for 45 min at 4 °C. Samples were acquired using the BD FACS Calibur flow cytometer.

Calcium flux assay

For measurement of intracellular calcium, CH27 cells transfected with vector or Y353F were loaded with 1 μM INDO-1-AM (Invitrogen) and equal volume of pluronic F-127 (Invitrogen) for 45 min at 37 °C. The cells were washed and resuspended in DMEM medium supplemented with 1% BSA and 20 mM HEPES. The cells were maintained in the dark at room temperature and a ratio of UV450/525 nm was recorded to establish the baseline fluorescence for unstimulated cells. Cells were stimulated at 30 s with 10 μg/ml of anti-IgM, and the UV450/525 ratio was recorded for 200 s. Samples were acquired using a BD LSRII flow cytometer and data were analyzed using FlowJo (Treestar).

Immunofluorescence microscopy

To visualize the BCR CH27 cells were stimulated with biotin-conjugated anti-IgM, fixed with 4% PFA, blocked with PBS containing 15% goat serum for 30 min followed by permeabilization and staining with AlexaFluor 488/633-conjugated Streptavidin (Molecular Probes) for 45 min at 4 °C. Next, the cells were stained with the pY353 antibody overnight at 4 °C and AlexaFluor 568-conjugated anti-rabbit IgG (Molecular Probes) for 30 min. Purified splenic B cells from B6 mice were stimulated with anti-IgM, fixed, permeabilized and stained with pThrERM antibody overnight, and AlexaFluor 568-conjugated anti-rabbit IgG for 30 min. Ezrin-YFP or Y353F-YFP transfected CH27 cells were stimulated and stained for the BCR as described above. For simultaneous imaging of pJNK and Y353-

phosphorylated ezrin, cells were stimulated, fixed and stained with pY353 antibody as described above, followed by staining with monoclonal antibody to pJNK and AlexaFluor 488/647-conjugated anti-mouse IgG (Molecular Probes) for 30 min at 4 °C. To mark the endosomal compartments, CH27 or splenic B cells were stained with antibodies to EEA1 (Invitrogen) or LAMP1 (BD Pharmingen) for 1 h at 4 °C followed by AlexaFluor 488-conjugated anti-chicken IgG (Molecular Probes) or AlexaFluor 633-conjugated anti-rat IgG (Molecular Probes), respectively for 45 min. The cells were stained with DAPI (Invitrogen), washed and image slices were acquired through the z-axis with an interval of 0.2 μm. Images were acquired using a Leica-AM TIRF microscope DMI6000 (Leica Microsystems) with an attached Hamamatsu EM-CCD camera, using HCX PL APO 100X oil objective at an additional 1.6× magnification with numerical aperture of 1.47 and appropriate filter cubes. Imaging was performed using the Leica acquisition software LAS AF Version 2.2.0. For Figure 3, CH27 cells were stained with antibodies to pY353, BCR and DAPI as described above, imaged by confocal microscopy and image slices were acquired through the z-axis with an interval of 0.1 μm. Images were acquired using a Perkin Elmer UltraVIEW VoX confocal imaging system and a Leica-AM microscope DMI6000 SD (Leica Microsystems) with an attached Hamamatsu EM-CCD C9100-50 camera, using HCX PL APO 100X oil objective with numerical aperture of 1.47 and appropriate filter cubes. Images were acquired using the Volocity 5.5 software.

Image analysis

The images across the z-series were combined using the Volocity Version 6.0.1 for 3D volumetric rendition of z-stacks. The z-stacks of images were digitally deconvolved using the ‘iterative restoration’ function in Volocity. Briefly, point spread functions were calculated for each fluorochrome channel and restoration was performed using 85–95% confidence limits and 25–30 iterations. For co-localization analysis, the deconvolved images were thresholded and Pearson’s correlation coefficients calculated for the specified pairs of channels across the stack of images using Volocity. For Fig. 7E, Metamorph image analysis software was used for digital “nearest-neighbors” deconvolution of the Z-stacks. ImagePro 6.1 software was used to quantify pixel intensity in Fig. 7F. Briefly, Z-stack images were analyzed using an algorithm written to quantify the number of green (pJNK) pixels in the region of interest. The images were filtered to enhance/equalize their appearance, thresholded, and the total number of green pixels in each region of interest were calculated by summing the segmented pixels in the region of interest across the stack of images.

Statistical analyses

Exact *p* values were calculated using the non-parametric two-tailed Mann-Whitney test except in Figure 1A and Figure 11B where unpaired t test was used. *p* values of less than 0.05, 0.01 and 0.001 are indicated as *, ** and ***, respectively. The tests were performed with 95% confidence interval (alpha level 0.05) using Prism4 (GraphPad). Mean±SD is reported along with *p* values.

RESULTS

BCR-specific tyrosine phosphorylation of ezrin

We first tested whether B cell stimulation would lead to phosphorylation of ezrin at Y353. Purified splenic B cells from B6 mice were treated with anti-mouse IgM, anti-CD40, lipopolysaccharide or CXCL13 at 37 °C for indicated time periods. Out of the four stimuli tested only BCR ligation induced phosphorylation of Y353 in ezrin (Fig. 1A). In contrast, all the ligands induced dephosphorylation of the conserved T567 (Fig. 1B). Phosphorylation of Y353 upon BCR crosslinking indicated that ezrin might have a second role in BCR

signaling in addition to its membrane-cytoskeleton tethering function that is known to regulate BCR diffusion and microclustering.

Phosphorylation of ezrin at Y353 requires Syk tyrosine kinase activity

As Lyn is the predominant Src family kinase (SFK) in B cells, we used B cells from B6 or $Lyn^{-/-}$ mice to determine whether it is required for Y353 phosphorylation in response to BCR crosslinking. Absence of Lyn kinase reduced the antigen-dependent tyrosine phosphorylation of ezrin (Fig. 2A). On the other hand, pretreatment of splenic B cells with the SFK inhibitor, PP1 abolished global tyrosine phosphorylation as well as phosphorylation of Y353 in ezrin (Supplementary Fig. S1A). These data suggest that SFK activity initiates the signaling events leading upto Y353 phosphorylation and that Lyn contributes to it but is not essential. SFK-mediated phosphorylation of ITAM in Igα and Igβ further initiates sequential activation of downstream tyrosine kinases such as Syk and Btk (2). As Lyn deficiency did not eliminate Y353 phosphorylation of ezrin, we tested if Syk or Btk played a role in phosphorylation of ezrin at Y353. For this we employed the chicken DT40 B cell lines with genetic deletions of Lyn, Syk or Btk. Wild type and Lyn, Syk or Btk-deficient DT40 B cells were stimulated with anti-IgM for the indicated times and induction of Y353 phosphorylation of ezrin was compared. Like Lyn-deficient murine B cells (Fig. 2A), Lyn-deficient DT40 cells showed reduced Y353 phosphorylation of ezrin (Fig. 2B). Btk deficiency did not affect Y353 phosphorylation whereas absence of Syk completely abrogated it (Fig. 2B) showing that Syk tyrosine kinase activity is necessary for phosphorylation of ezrin at Y353. Treatment of mouse splenic B cells with a Syk kinase inhibitor, piceatannol also resulted in a dose-dependent inhibition of Y353 phosphorylation (Supplementary Fig. S1B). As phosphorylation of Syk was reduced and not completely abrogated in the absence of Lyn (Supplementary Fig. S1C), the remaining Y353 phosphorylation of ezrin in Lyn-deficient B cells may be due to the residual Syk activity.

Protein kinases are known to interact with their substrates during the phosphorylation event. Therefore, we tested if Syk interacts with ezrin to phosphorylate it at Y353. Ezrin co-immunoprecipitated with Syk from lysates of CH27 cells regardless of whether the cells were stimulated with anti-IgM or not (Fig. 2C). However, the association of Y353-phosphorylated ezrin with Syk was maximal at 1 min (Fig. 2C), which coincides with the peak of Y353 phosphorylation observed in B cell lysates (Fig. 1A). These results indicate that ezrin and Syk exist in a preformed complex that facilitates Syk-mediated phosphorylation at Y353 upon BCR stimulation.

Tyrosine-phosphorylated ezrin co-localizes with the BCR

The interaction between ezrin and Syk suggested that Y353-phosphorylated ezrin may be part of the BCR signalosome that assembles at the membrane and supports antigen-induced early signaling events. We employed confocal microscopy to determine the subcellular localization of Y353-phosphorylated ezrin with respect to the BCR in CH27 cells using antibodies to pY353 and BCR. Unstimulated B cells showed punctate distribution of the BCRs at the plasma membrane and negligible signal for Y353-phosphorylated ezrin (Fig. 3A). Anti-IgM stimulation induced tyrosine phosphorylation of ezrin at 1 min showing a scattered, punctate distribution with patches of co-localization with the BCR. At 10 min of anti-IgM stimulation the BCRs appeared focused and Y353-phosphorylated ezrin co-localized with the BCR. The BCR and Y353-phosphorylated ezrin localized to the perinuclear space and remained co-localized upto 30 min of stimulation. The perinuclear co-localization at later times of anti-IgM stimulation was observed in more than 80% of the B cells imaged (Fig. 3B).

BCR crosslinking induces receptor oligomerization and generation of signaling microclusters or "microsignalosomes". The endocytosed antigen-bound BCRs traffic through early and late endosomes to deliver the antigen for proteolytic processing and transfer onto the MHC II molecules (20). As Y353-phosphorylated ezrin co-localized with the BCR in the perinuclear region, we examined if it traffics through the endosomal compartments together with the BCR. We imaged Y353-phosphorylated ezrin and BCR along with EEA1 and LAMP1, membrane proteins that mark early and late endosomes, respectively. CH27 cells were stimulated with anti-IgM and immunostained with antibodies to pY353, BCR and EEA1 (Fig. 4A, B) or LAMP1 (Fig. 5A, B). In order to clearly visualize the subcellular localization of Y353-phosphorylated ezrin and BCR we generated volumetric reconstructions of each cell using z-stacks of the images. Resting B cells showed punctate distribution of the BCRs, negligible tyrosine-phosphorylated ezrin and scattered distribution of EEA1-positive early endosomes (Fig. 4A). Anti-IgM-induced Y353-phosphorylated ezrin appeared scattered at 5 min of stimulation and was co-localized in patches with the BCR-containing EEA1-positive early endosomes (Fig. 4A, B). At 10 min of anti-IgM stimulation, BCR and Y353-phosphorylated ezrin were co-localized, with a few patches still associating with EEA1-positive endosomes (Fig. 4A, B). BCR and Y353-phosphorylated ezrin remained co-localized at 15 min and 30 min of stimulation as seen in Fig. 3A but were mostly outside the EEA1-positive endosomes at these times (Fig. 4A, B). Imaging of the BCR, Y353-phosphorylated ezrin and the late endosomal protein, LAMP1 showed negligible association of BCR and Y353-phosphorylated ezrin with LAMP1 at 5 min of anti-IgM stimulation (Fig. 5A). Significant co-localization of the BCR and Y353-phosphorylated ezrin with LAMP1 was observed starting at 10 min that further increased at 30 min (Fig. 5A, B). Together, these results show that within minutes of BCR crosslinking Y353-phosphorylated ezrin and the BCR co-localized in EEA1-positive endosomes and remained co-localized in LAMP1-positive endosomes at later times of stimulation.

Recovery of threonine phosphorylation of ezrin occurs at the plasma membrane and in late endosomes

Anti-IgM-induced dephosphorylation of ezrin and moesin at the regulatory threonine residue is transient, as rephosphorylation is observed at 30 min of stimulation (Fig. 1B). At this time, Y353-phosphorylated ezrin is observed within late endosomes (Fig. 4, 5). To identify the intracellular compartment where ezrin becomes rephosphorylated at the threonine residue, we imaged pThrERM together with LAMP1 in B cells stimulated with anti-IgM over a longer time period. Rapid loss of pThrERM from the plasma membrane was observed at 3 and 10 min of stimulation (Fig. 6A, B). Most of the recovery of pThrERM occurred at the plasma membrane starting at 20 min of anti-IgM stimulation (Fig 6A, B), however, significant co-localization of pThrERM was also detected with LAMP1 at 30 min of stimulation (Fig. 6A, C), indicating that a pool of ezrin located within late endosomes also undergoes threonine phosphorylation.

Expression of the Y353F mutant of ezrin specifically inhibits JNK activation

To investigate the function of Y353 phosphorylation of ezrin in BCR signaling we mutated Y353 to phenylalanine (Y353F) in the plasmid vector pIRES-2-EGFP (pI2E). Bicistronic expression of EGFP was used as a reporter of transfection efficiency. The expression of IgM was equivalent in CH27 cells transfected with vector or the Y353F mutant (Supplementary Fig. S2A). As Y353-phosphorylated ezrin co-localized with the BCR in endosomes within 5 min of stimulation, we first tested if expression of the Y353F mutant altered stimulation-induced BCR internalization in CH27 cells transiently transfected with the vector pI2E (referred to as vector) or pI2E-Y353F (referred to as Y353F). Anti-IgM-induced BCR internalization was unaltered in the presence of the Y353F mutant of ezrin (Supplementary Fig. S2B). Expression of the Y353F mutant also did not alter anti-IgM-induced calcium flux

(Fig. 7A). Next, CH27 cells expressing the vector or Y353F were stimulated with anti-IgM for indicated times and lysates probed with antibodies to phosphorylated forms of key signaling intermediates in BCR activation. As the Y353F mutant of ezrin is untagged, expression of the Y353F mutant was assessed by increase in intensity of the protein band corresponding to endogenous ezrin in the immunoblot (Fig. 7B, bottom panel). The phosphorylation of BLNK and PLCγ2, two proteins that participate early in the BCR signaling cascade, was unaltered in the presence of the Y353F mutant of ezrin (Fig. 7B). ERK1/2 phosphorylation also remained intact in CH27 cells expressing the Y353F mutant of ezrin (Fig. 7C), whereas anti-IgM-induced phosphorylation of both the p54 and p46 isoforms of JNK was markedly inhibited (Fig. 7D). A prominent non-specific band of 43 kDa was observed below the p46 isoform of phosphorylated JNK (Fig. 7D), but its intensity was similar between the vector and Y353F expressing cells (Supplementary Fig. S2C). To confirm the effect of Y353F mutant on JNK activation, we employed immunofluorescence microscopy to image the active, phosphorylated form of JNK (pJNK) in vector and Y353F expressing CH27 cells stimulated with anti-IgM. Consistent with the data in Fig. 7D, anti-IgM stimulation of CH27 cells transfected with vector alone induced phosphorylation of JNK (Fig. 7E, F). In contrast, anti-IgM-induced phosphorylation of JNK was markedly reduced in cells expressing the Y353F mutant of ezrin (Fig. 7E, F). These data suggest that tyrosine phosphorylation of ezrin positively regulates JNK activation.

Y353-phosphorylated ezrin co-localizes with phosphorylated JNK within endosomal compartments

Intracellular MAPK signaling depends on their compartmentalization with the BCR within endosomes (8). As Y353-phosphorylated ezrin and the BCR co-migrated in endosomes we considered the possibility that tyrosine-phosphorylated ezrin spatially localizes JNK in proximity to the BCR. To investigate whether Y353-phosphorylated ezrin co-localizes with the active, phosphorylated form of JNK, we imaged Y353-phosphorylated ezrin and pJNK using immunofluorescence microscopy. CH27 cells were stimulated with anti-IgM, and immunostained with antibodies to pY353 and pJNK and the endosomal proteins EEA1 and LAMP1. Unstimulated B cells showed minimal signal for pJNK and Y353-phosphorylated ezrin (Fig. 8A). Anti-IgM stimulation resulted in Y353 phosphorylation of ezrin and JNK phosphorylation and both showed a scattered distribution at 1 min of stimulation (Fig. 8A). The co-localization of Y353-phosphorylated ezrin and pJNK increased significantly at 10 and 30 min of anti-IgM stimulation (Fig. 8B), and the Y353-phosphorylated ezrin-pJNK complex began to appear more focused at 30 min (Fig. 8A). The co-localization of Y353-phosphorylated ezrin-pJNK complex with EEA1-positive early endosomes peaked at 10 min of stimulation and decreased by 30 min (Fig. 8A, B). The Y353-phosphorylated ezrin-pJNK complexes started associating with the LAMP1-positive late endosomes at 10 min of stimulation and were maximally co-localized at 30 min (Fig. 9A, B).

Ezrin physically associates with JNK and MKK7

JNK-interacting proteins (JIPs) are scaffolds that facilitate JNK signal transduction by physically interacting with JNK and its upstream kinases such as MLK and MKK 7 to bring them into close proximity for serial phosphorylation (21, 22). JIPs are poorly expressed in B cells (23) and their contribution towards BCR-dependent JNK activation has not been explored. We considered the possibility that Y353-phosphorylated ezrin regulates JNK activation in a JIP-like manner. Therefore, we examined the interaction between Y353-phosphorylated ezrin and JNK in anti-IgM stimulated B cells by precipitating JNK from CH27 cells stimulated with anti-IgM using GST-c-Jun fusion protein-conjugated Sepharose beads, and looking for the presence of co-precipitated Y353-phosphorylated ezrin. Y353-phosphorylated ezrin associated with JNK at 5 min of anti-IgM stimulation and the association peaked at 10 min (Fig. 10A). Next, we examined the association of ezrin with

MKK7, one of the upstream kinases that directly phosphorylates JNK. Maximal association between tyrosine-phosphorylated ezrin and MKK7 was detected at 5 min of BCR stimulation (Fig. 10B).

Y353F mutant of ezrin shows reduced co-localization with the internalized BCR

In order to address the possibility that the non-phosphorylatable Y353F mutant of ezrin may display altered co-localization or co-trafficking with the BCR or phosphorylated JNK, we created a tagged version of the Y353F mutant in which YFP was attached to its C-terminus (Y353F-YFP). This tagged fusion protein allowed us to distinguish between the ectopic Y353F mutant ezrin and the endogenous wild type ezrin. As expected, the Y353F-YFP mutant did not undergo Y353 phosphorylation upon anti-IgM stimulation (Supplementary Fig. 2D). In view of the fact that phosphorylated JNK is significantly reduced in cells expressing the Y353F mutant (Fig. 7E), it was difficult to gain useful information about co-localization of pJNK and Y353F-YFP. Therefore, we visualized the BCR together with Ezrin-YFP or Y353F-YFP. As the BCR and ezrin localize to the plasma membrane and cortical region, respectively, co-localization between the two was observed in unstimulated B cells (Fig. 11A, B). The extent of co-localization of the Y353F-YFP with the BCR was higher than that observed for Ezrin-YFP in unstimulated B cells (Fig. 11B). In contrast, at 1 and 10 min of stimulation when the BCR traffics to early and late endosomes, Y353F-YFP co-localized less well with the BCR as compared to Ezrin-YFP (Fig. 11A, B). It is important to note that this experiment relies on detection of co-localization between the BCR and a small proportion of ectopically expressed ezrin that undergoes tyrosine phosphorylation. Nonetheless, as Y353F-YFP does not get tyrosine phosphorylated, reduction in its co-segregation with the internalized BCR suggests its inability to link with the endosomal BCR signalosome. Taken together, our data indicate that Y353-phosphorylated ezrin functions as an adaptor to spatially localize the JNK signaling module in the vicinity of the BCR signalosome.

DISCUSSION

In this study we expand the role of ezrin in B cells beyond its established role as a linker protein between the plasma membrane and actin cytoskeleton. In addition to dephosphorylation of T567, ezrin undergoes Syk-dependent phosphorylation at Y353 upon BCR crosslinking. BCR stimulation-induced increase in association of Y353-phosphorylated ezrin with JNK and its kinase MKK7, and its increased co-localization with the BCR and phosphorylated JNK within endosomal compartments point towards an adaptor function for Y353-phosphorylated ezrin in JNK activation.

Stimulation of naïve B cells with ligands that engage different receptors on B cells induces various functional outcomes including proliferation, survival and migration. It is known that B cell proliferation downstream of BCR, TLR4 or CD40 ligation, as well as B cell migration induced by CXCL13 involve polarization of intracellular signaling molecules, and require morphological and cytoskeletal reorganization (24–27). Dephosphorylation of the regulatory T567 in ezrin by all the ligands tested in our study suggests a common and conserved mechanism of conformational inactivation that may facilitate membrane-cytoskeletal remodeling during proliferation and migration of B cells. Exclusive induction of Y353 phosphorylation of ezrin by BCR ligation indicated that Y353-phosphorylated ezrin has a specific function in antigen-dependent B cell activation. Previously, CD81 but not BCR or CD19 crosslinking was reported to induce Y353 phosphorylation in human B cell lines (19). BCR-mediated Y353 phosphorylation was not observed in the OCI-Ly8 DLBCL cell line in that study, possibly due to the lower dose of stimulus and longer stimulation time (30 min) (19). In our study, Y353 phosphorylation of ezrin was still detectable at 30 min of anti-IgM stimulation, but it was much lower than that observed at 1 min. We have previously shown

that anti-IgM stimulation induces rapid, but transient loss of T567 phosphorylation of ezrin that is recovered later (10). The rephosphorylation of ezrin at T567 in late endosomes indicates that it may reconnect with the actin cytoskeleton in this compartment as well, and recycle back to the plasma membrane. Ezrin is known to facilitate recycling of the alpha1-adrenergic receptor (28) in an actin-dependent manner.

Activation of the Src family tyrosine kinases is the earliest event in the BCR crosslinking-mediated signaling cascade, and accordingly lack of Lyn lowered Y353 phosphorylation of ezrin. Furthermore, an absolute requirement of Syk kinase activity for Y353 phosphorylation of ezrin was observed in the Syk-deficient DT40 B cells. The residual Y353 phosphorylation observed in Lyn-deficient mouse B cells (Fig. 2A) and DT40 chicken B cell line (Fig. 2B) suggests that Fyn and/or Blk cooperate with Lyn to transduce the signal to Syk. Notably, CD81-dependent Y353 phosphorylation of ezrin was also shown to be Syk-dependent (19). Although CD40 and CXCR5 engagement synergize with BCR-crosslinking to enhance Syk kinase activation, independently these stimuli induce negligible activation of Syk (27, 29). This correlates well with our observations of insignificant Y353 phosphorylation of ezrin in B cells stimulated with their ligands, anti-CD40 and CXCL13. The form of ezrin that associates with Syk (Fig. 2C) in unstimulated naive B cells may either be the conformationally active fraction bound to the phosphoprotein associated with glycosphingolipid-enriched microdomains (PAG/Cbp) or the dormant fraction that can co-exist in the cytosol (Fig. 11C). Interestingly, ERM proteins were reported to associate with Syk through a putative ITAM-like sequence in their FERM domain during P-selectin glycoprotein ligand (PSGL)-1-induced transcriptional activation in T cells (30). The mode of association of ezrin with Syk in B cells remains to be tested. As the Y353 residue is not conserved in moesin, the ability of ezrin to regulate JNK activation may not be redundant with moesin.

Pervanadate stimulation of murine $CD4^+$ T cells, but not TCR engagement alone, was reported to induce Y353 phosphorylation of ezrin but its function remains unidentified (13). Ezrin was shown to associate with and recruit the tyrosine kinase ZAP-70 to the immunological synapse in T cells (31). Both ZAP-70 and Syk belong to the Syk family of cytoplasmic non-receptor tyrosine kinases that are involved in antigen receptor-mediated signaling in T and B cells, respectively. Given the functional similarities between ZAP-70 and Syk, and their role in antigen-mediated signaling, ZAP-70 may catalyze Y353-phosphorylation of ezrin at the immunological synapse in T cells. In a separate study, TCR ligation in human T cell lines was shown to induce tyrosine-phosphorylation of ezrin in an Lck and ZAP-70-dependent manner (32), however the site of tyrosine-phosphorylation in ezrin was not identified.

BCR “microsignalosomes” assemble at the surface of B cells and include intracellular signaling molecules such as Syk, PLCγ2 and Vav (33). As BCR signaling proceeds, intracellular proteins sequentially enter and exit the BCR signaling complex. Continual signal transduction by the internalized BCRs within endosomes underscores the importance of compartmentalization of signaling components in optimal regulation of the MAPK pathways (8). Preventing BCR endocytosis and its subsequent sequential co-localization with kinases within the endosomes was shown to alter the extent and outcome of MAPK activation (8). Recent studies have identified MAPK scaffold proteins e.g. MP1 and β-arrestin that modulate stimulus-dependent activation of ERK and JNK signaling pathways by spatially localizing signaling modules to endosomes (34, 35). Interestingly, the prominent perinuclear co-localization of Y353-phosphorylated ezrin with the BCR and pJNK at later times of B cell stimulation resembles the localization reported for JNK scaffolds in fibroblasts and neuronal cells (36). The major groups of JNK scaffolds are the JIP proteins of which JIP-1 and 2 are almost exclusively expressed in neuronal cells (23, 37). Follicular

B cells express very low levels of JIP3 and JIP4, of which JIP4 was shown to facilitate the activation of p38 instead of JNK (23, 38). Our data show association of ezrin with JNK and MKK7, indicating that ezrin may substitute for JIPs and act as a JNK scaffold in B cells. Our immunoprecipitation data showed that Y353-phosphorylated ezrin and JNK associated maximally at 10 min and dissociated at later times of stimulation. However, we continued to observe the co-localization of Y353-phosphorylated ezrin and pJNK within late endosomes at 30 min suggesting that the physical interaction between Y353-phosphorylated ezrin and JNK or MKK7 may be a transient requirement and serve to spatially localize these kinases within the BCR-occupied signaling endosomes. Y353-phosphorylated ezrin may either associate directly with MKK7 and JNK, and function as a JIP-like adaptor or facilitate the function of another as yet unidentified JNK scaffold protein. Our data using the YFP-tagged fusion proteins indicate that BCR internalization was unaffected in the presence of Y353F-YFP. Interestingly, the region around the internalized BCR was found to be rich in Ezrin-YFP but devoid of Y353F-YFP, which indicates the importance of Y353 phosphorylation in recruiting ezrin to the endosomal compartment. Our biochemical and microscopy analyses show impaired JNK activation upon expression of the Y353F mutant of ezrin confirming the requirement of Y353-phosphorylation of ezrin. Our data also suggest that the Y353F mutant acts in a dominant negative manner, and further characterization of its protein-protein interactions will reveal the mechanism by which it interferes with the ability of endogenous ezrin to facilitate JNK activation.

Y353-phosphorylated ezrin has been reported to regulate the survival of non-hematopoetic cells (39). Expression of the Y353F mutant of ezrin in kidney epithelial cells led to increased apoptosis that was attributed to decrease in association of ezrin with the p85 subunit of PI3K and impaired activation of Akt downstream of PI3K (39). Ezrin is highly expressed in HS2 leukemic stage cell lines of proerythroblastic cells, and overexpression of the Y353F mutant of ezrin leads to increased cell death, supporting a role for Y353-phosphorylated ezrin in enhancing cell survival (40). These studies and ours suggest that ezrin can partner with different signaling proteins depending on the cellular context and stimulus.

Finally, our data suggest a model wherein BCR crosslinking induces activation of Syk leading to Y353 phosphorylation of ezrin (Fig. 11C). Y353-phosphorylated ezrin accesses and associates with JNK and MKK7 and couples proximal BCR signaling with the JNK signaling module within endosomes (Fig. 11C). As the BCR continues to transduce signals in the endosomal compartment it supports JNK activation. Moreover, ezrin undergoes resphosphorylation at T567 in both the $LAMP^+$ compartment and at the plasma membrane. Therefore, we propose that Y353-phosphorylated ezrin functions as an adaptor to recruit JNK and MKK7 spatially close to the active BCR within endosomes. In conclusion, we have identified Y353-phosphorylated ezrin as a novel regulator of JNK signaling in antigen-activated B cells.

Supplementary Material

Refer to Web version on PubMed Central for supplementary material.

Acknowledgments

The authors would like to thank the Lerner Research Institute Imaging Core personnel and Dr. Amit Vasanji for assistance with imaging and image analysis.

REFERENCES

1. DeFranco AL. The complexity of signaling pathways activated by the BCR. Curr Opin Immunol. 1997; 9:296–308. [PubMed: 9203421]
2. Dal Porto JM, Gauld SB, Merrell KT, Mills D, Pugh-Bernard AE, Cambier J. B cell antigen receptor signaling 101. Mol Immunol. 2004; 41:599–613. [PubMed: 15219998]
3. Batista FD, Treanor B, Harwood NE. Visualizing a role for the actin cytoskeleton in the regulation of B-cell activation. Immunol Rev. 2010; 237:191–204. [PubMed: 20727037]
4. Pierce SK, Liu W. The tipping points in the initiation of B cell signalling: how small changes make big differences. Nat Rev Immunol. 2010; 10:767–777. [PubMed: 20935671]
5. Treanor B, Depoil D, Gonzalez-Granja A, Barral P, Weber M, Dushek O, Bruckbauer A, Batista FD. The membrane skeleton controls diffusion dynamics and signaling through the B cell receptor. Immunity. 2010; 32:187–199. [PubMed: 20171124]
6. Depoil D, Fleire S, Treanor BL, Weber M, Harwood NE, Marchbank KL, Tybulewicz VL, Batista FD. CD19 is essential for B cell activation by promoting B cell receptor-antigen microcluster formation in response to membrane-bound ligand. Nat Immunol. 2008; 9:63–72. [PubMed: 18059271]
7. Siemasko K, Eisfelder BJ, Stebbins C, Kabak S, Sant AJ, Song W, Clark MR. Ig alpha and Ig beta are required for efficient trafficking to late endosomes and to enhance antigen presentation. J Immunol. 1999; 162:6518–6525. [PubMed: 10352267]
8. Chaturvedi A, Martz R, Dorward D, Waisberg M, Pierce SK. Endocytosed BCRs sequentially regulate MAPK and Akt signaling pathways from intracellular compartments. Nat Immunol. 2011; 12:1119–1126. [PubMed: 21964606]
9. Fehon RG, McClatchey AI, Bretscher A. Organizing the cell cortex: the role of ERM proteins. Nat Rev Mol Cell Biol. 2010; 11:276–287. [PubMed: 20308985]
10. Gupta N, Wollscheid B, Watts JD, Scheer B, Aebersold R, DeFranco AL. Quantitative proteomic analysis of B cell lipid rafts reveals that ezrin regulates antigen receptor-mediated lipid raft dynamics. Nat Immunol. 2006; 7:625–633. [PubMed: 16648854]
11. Parameswaran N, Matsui K, Gupta N. Conformational switching in ezrin regulates morphological and cytoskeletal changes required for B cell chemotaxis. J Immunol. 2011; 186:4088–4097. [PubMed: 21339367]
12. Treanor B, Depoil D, Bruckbauer A, Batista FD. Dynamic cortical actin remodeling by ERM proteins controls BCR microcluster organization and integrity. J Exp Med. 2011; 208:1055–1068. [PubMed: 21482698]
13. Shaffer MH, Dupree RS, Zhu P, Saotome I, Schmidt RF, McClatchey AI, Freedman BD, Burkhardt JK. Ezrin and moesin function together to promote T cell activation. J Immunol. 2009; 182:1021–1032. [PubMed: 19124745]
14. Pearson MA, Reczek D, Bretscher A, Karplus PA. Structure of the ERM protein moesin reveals the FERM domain fold masked by an extended actin binding tail domain. Cell. 2000; 101:259–270. [PubMed: 10847681]
15. Zhou R, Cao X, Watson C, Miao Y, Guo Z, Forte JG, Yao X. Characterization of protein kinase A-mediated phosphorylation of ezrin in gastric parietal cell activation. J Biol Chem. 2003; 278:35651–35659. [PubMed: 12840026]
16. Crepaldi T, Gautreau A, Comoglio PM, Louvard D, Arpin M. Ezrin is an effector of hepatocyte growth factor-mediated migration and morphogenesis in epithelial cells. J Cell Biol. 1997; 138:423–434. [PubMed: 9230083]
17. Krieg J, Hunter T. Identification of the two major epidermal growth factor-induced tyrosine phosphorylation sites in the microvillar core protein ezrin. J Biol Chem. 1992; 267:19258–19265. [PubMed: 1382070]
18. Heiska L, Melikova M, Zhao F, Saotome I, McClatchey AI, Carpen O. Ezrin is key regulator of Src-induced malignant phenotype in three-dimensional environment. Oncogene. 2011; 30:4953–4962. [PubMed: 21666723]
19. Coffey GP, Rajapaksa R, Liu R, Sharpe O, Kuo CC, Krauss SW, Sagi Y, Davis RE, Staudt LM, Sharman JP, Robinson WH, Levy S. Engagement of CD81 induces ezrin tyrosine phosphorylation

and its cellular redistribution with filamentous actin. J Cell Sci. 2009; 122:3137–3144. [PubMed: 19654214]

20. Siemasko K, Clark MR. The control and facilitation of MHC class II antigen processing by the BCR. Curr Opin Immunol. 2001; 13:32–36. [PubMed: 11154914]
21. Engstrom W, Ward A, Moorwood K. The role of scaffold proteins in JNK signalling. Cell Prolif. 2010; 43:56–66. [PubMed: 19922489]
22. Morrison DK, Davis RJ. Regulation of MAP kinase signaling modules by scaffold proteins in mammals. Annu Rev Cell Dev Biol. 2003; 19:91–118. [PubMed: 14570565]
23. Lattin JE, Schroder K, Su AI, Walker JR, Zhang J, Wiltshire T, Saijo K, Glass CK, Hume DA, Kellie S, Sweet MJ. Expression analysis of G Protein-Coupled Receptors in mouse macrophages. Immunome Res. 2008; 4:5. [PubMed: 18442421]
24. Thaunat O, Granja AG, Barral P, Filby A, Montaner B, Collinson L, Martinez-Martin N, Harwood NE, Bruckbauer A, Batista FD. Asymmetric segregation of polarized antigen on B cell division shapes presentation capacity. Science. 2012; 335:475–479. [PubMed: 22282815]
25. Duchez S, Rodrigues M, Bertrand F, Valitutti S. Reciprocal polarization of T and B cells at the immunological synapse. J Immunol. 2011; 187:4571–4580. [PubMed: 21930964]
26. Boisvert J, Edmondson S, Krummel MF. Immunological synapse formation licenses CD40-CD40L accumulations at T-APC contact sites. J Immunol. 2004; 173:3647–3652. [PubMed: 15356109]
27. Saez de Guinoa J, Barrio L, Mellado M, Carrasco YR. CXCL13/CXCR5 signaling enhances BCR-triggered B-cell activation by shaping cell dynamics. Blood. 2011; 118:1560–1569. [PubMed: 21659539]
28. Stanasila L, Abuin L, Diviani D, Cotecchia S. Ezrin directly interacts with the alpha1b-adrenergic receptor and plays a role in receptor recycling. J Biol Chem. 2006; 281:4354–4363. [PubMed: 16352594]
29. Ying H, Li Z, Yang L, Zhang J. Syk mediates BCR- and CD40-signaling integration during B cell activation. Immunobiology. 2011; 216:566–570. [PubMed: 21074890]
30. Urzainqui A, Serrador JM, Viedma F, Yanez-Mo M, Rodriguez A, Corbi AL, Alonso-Lebrero JL, Luque A, Deckert M, Vazquez J, Sanchez-Madrid F. ITAM-based interaction of ERM proteins with Syk mediates signaling by the leukocyte adhesion receptor PSGL-1. Immunity. 2002; 17:401–412. [PubMed: 12387735]
31. Ilani T, Khanna C, Zhou M, Veenstra TD, Bretscher A. Immune synapse formation requires ZAP-70 recruitment by ezrin and CD43 removal by moesin. J Cell Biol. 2007; 179:733–746. [PubMed: 18025306]
32. Tomas EM, Darlington PJ, Chau LA, Madrenas J. The role of ezrin in T-cell receptor-dependent signaling. Transplant Proc. 2001; 33:207–208. [PubMed: 11266781]
33. Harwood NE, Batista FD. Early events in B cell activation. Annu Rev Immunol. 2010; 28:185–210. [PubMed: 20192804]
34. McDonald PH, Chow CW, Miller WE, Laporte SA, Field ME, Lin FT, Davis RJ, Lefkowitz RJ. Beta-arrestin 2: a receptor-regulated MAPK scaffold for the activation of JNK3. Science. 2000; 290:1574–1577. [PubMed: 11090355]
35. Teis D, Taub N, Kurzbauer R, Hilber D, de Araujo ME, Erlacher M, Offterdinger M, Villunger A, Geley S, Bohn G, Klein C, Hess MW, Huber LA. p14-MP1-MEK1 signaling regulates endosomal traffic and cellular proliferation during tissue homeostasis. J Cell Biol. 2006; 175:861–868. [PubMed: 17178906]
36. Lee CM, Onesime D, Reddy CD, Dhanasekaran N, Reddy EP. JLP: A scaffolding protein that tethers JNK/p38MAPK signaling modules and transcription factors. Proc Natl Acad Sci U S A. 2002; 99:14189–14194. [PubMed: 12391307]
37. Dhanasekaran DN, Kashef K, Lee CM, Xu H, Reddy EP. Scaffold proteins of MAP-kinase modules. Oncogene. 2007; 26:3185–3202. [PubMed: 17496915]
38. Kelkar N, Standen CL, Davis RJ. Role of the JIP4 scaffold protein in the regulation of mitogen-activated protein kinase signaling pathways. Mol Cell Biol. 2005; 25:2733–2743. [PubMed: 15767678]

39. Gautreau A, Poullet P, Louvard D, Arpin M. Ezrin, a plasma membrane-microfilament linker, signals cell survival through the phosphatidylinositol 3-kinase/Akt pathway. Proc Natl Acad Sci U S A. 1999; 96:7300–7305. [PubMed: 10377409]

40. Monni R, Haddaoui L, Naba A, Gallais I, Arpin M, Mayeux P, Moreau-Gachelin F. Ezrin is a target for oncogenic Kit mutants in murine erythroleukemia. Blood. 2008; 111:3163–3172. [PubMed: 18182570]

ABBREVIATIONS

ERM	Ezrin-Radixin-Moesin
EEA1	Early Endosome Antigen 1
JIP	JNK-interacting protein
LAMP1	Lysosomal-Associated Membrane Protein 1
MKK7	MAPKK7
pI2E	pIRES-2-eGFP
pThrERM	phosphorylated threonine in ERM
SFK	Src family kinase
YFP	yellow fluorescent protein

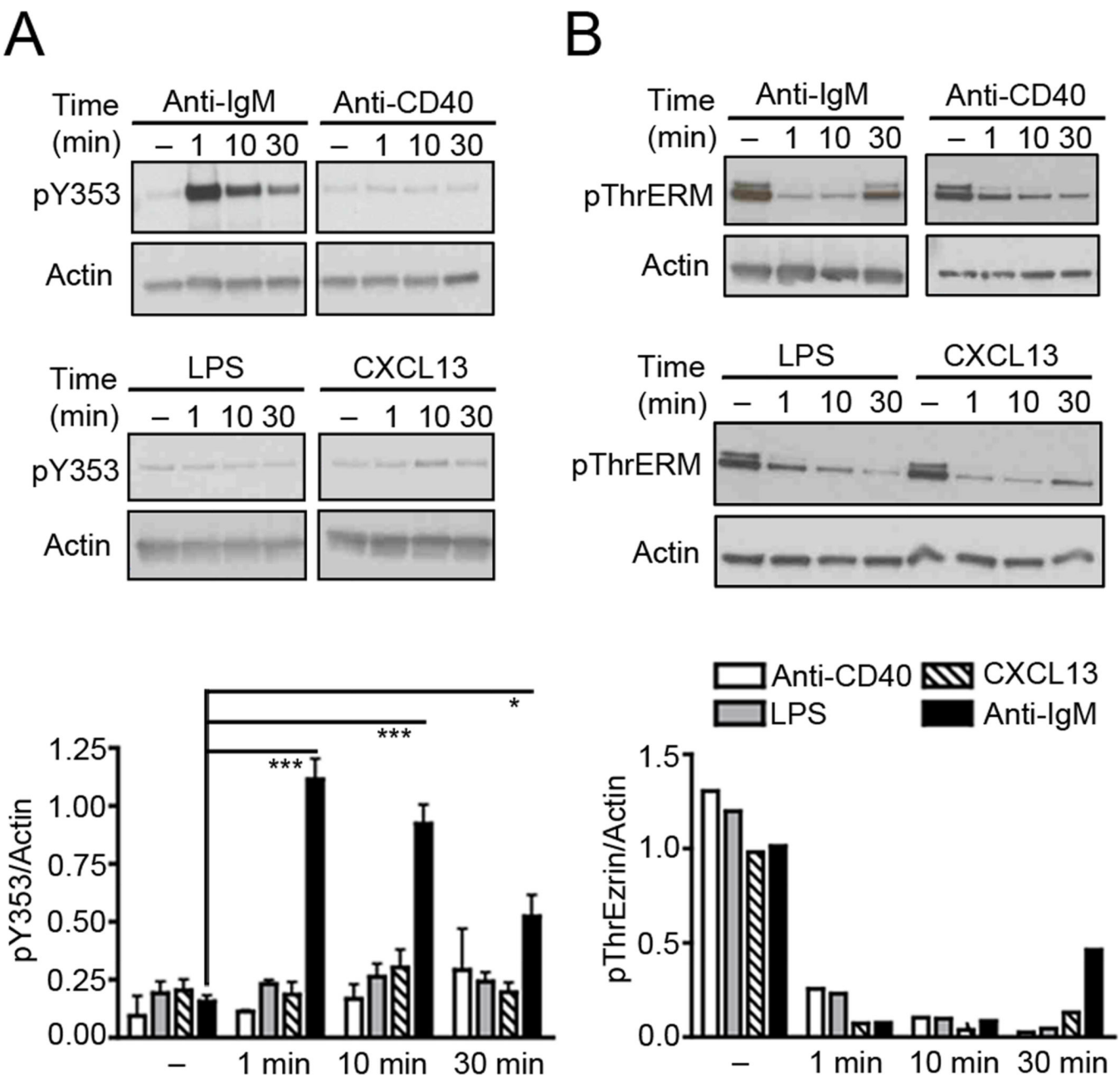

Figure 1. BCR stimulation induces phosphorylation of ezrin at Y353

Lysates from purified splenic B cells stimulated with 10 μg/ml of anti-IgM, 10 μg/ml of anti-CD40, 10 μg/ml of LPS or 3 μg/ml of CXCL13 were probed with antibodies to actin and **(A)** pY353 or **(B)** pThrERM. The bar graph in (A) shows the ratio of pY353 to actin (mean±SD) from three independent experiments. The data in (B) are representative of two independent experiments.

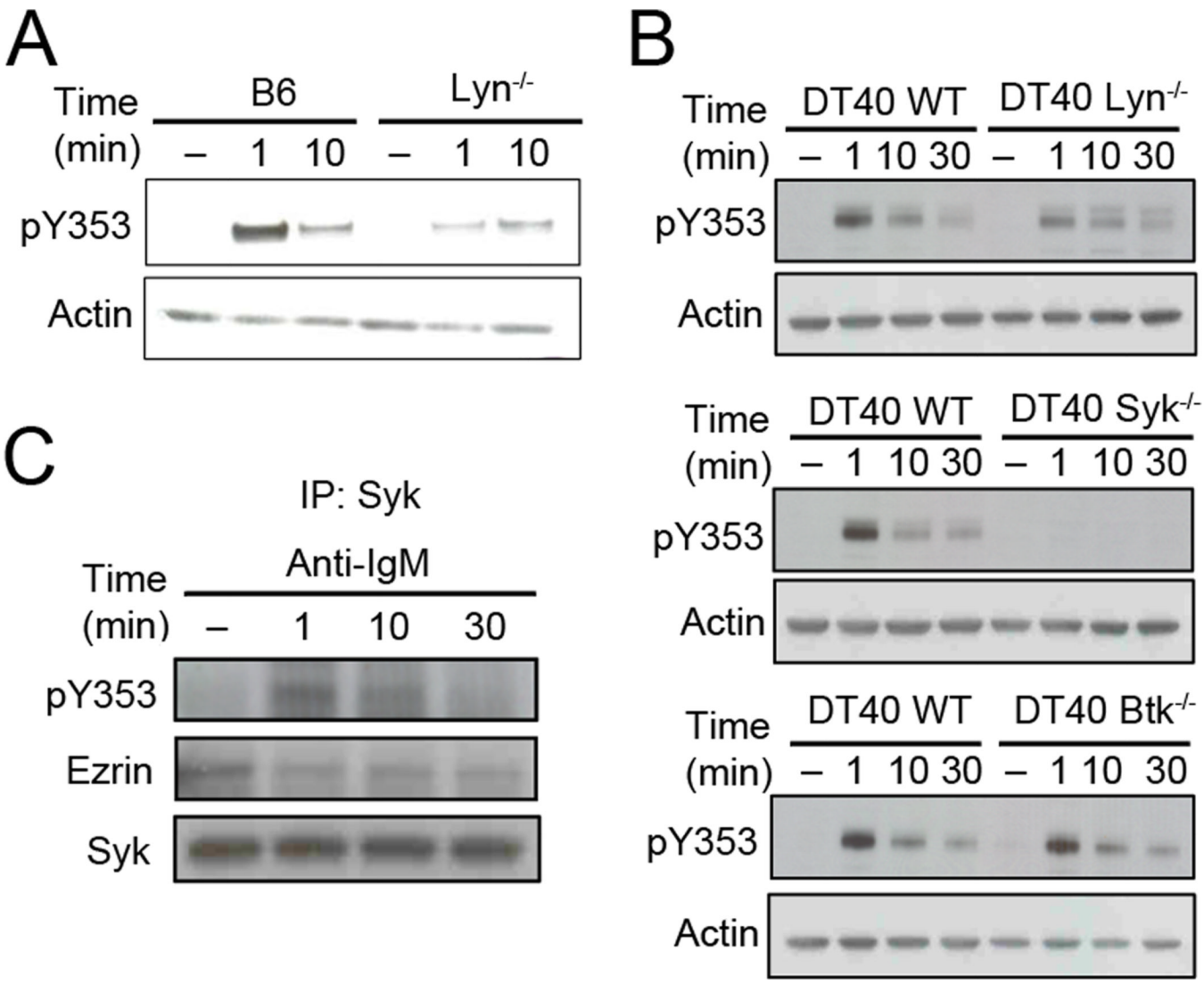

Figure 2. Y353 phosphorylation of ezrin requires Syk kinase activity

(A) Purified B cells from B6 or Lyn-deficient mice were stimulated with 10 μg/ml of anti-IgM for the indicated time and lysates probed with pY353 and actin antibody. The data are representative of two independent experiments. **(B)** Wild type or Lyn-, Syk-, or Btk-deficient DT40 B cells were stimulated with 10 μg/ml of anti-chicken IgM for the indicated time and lysates probed with pY353 and actin antibody. **(C)** CH27 B cells were lysed after stimulation with 10 μg/ml of anti-IgM, and subjected to Syk immunoprecipitation and immunoblotting with ezrin, pY353 or Syk antibodies. Data in (B) and (C) are representative of three independent experiments.

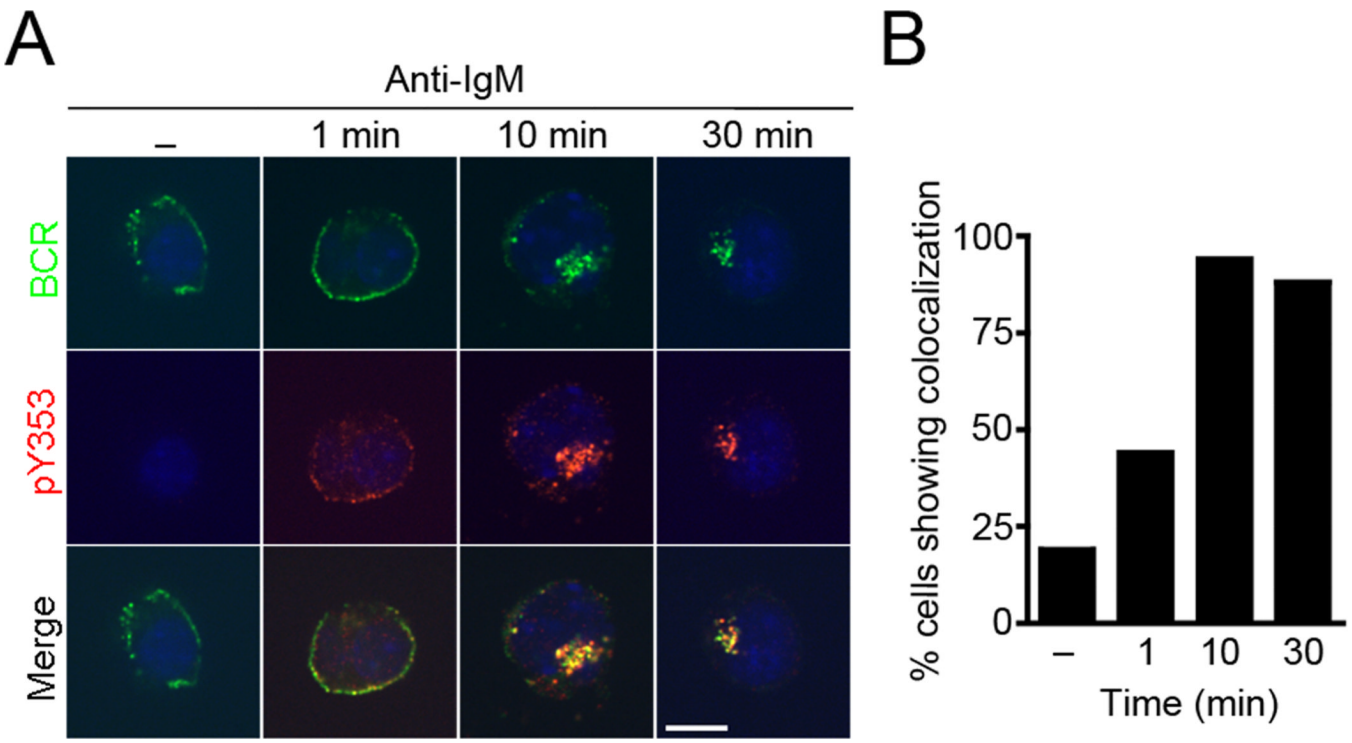

Figure 3. BCR stimulation induces co-localization of Y353-phosphorylated ezrin with the BCR

(A) CH27 B cells were stimulated with 10 μg/ml of anti-IgM for the indicated time, stained for Y353-phosphorylated ezrin (red), BCR (green), DAPI (blue) and imaged by confocal microscopy. Scale bar, 10 μm. The data are representative of two independent experiments (n=15 cells per group). **(B)** Percentage of cells that display co-localization of Y353-phosphorylated ezrin with the BCR at different times of stimulation.

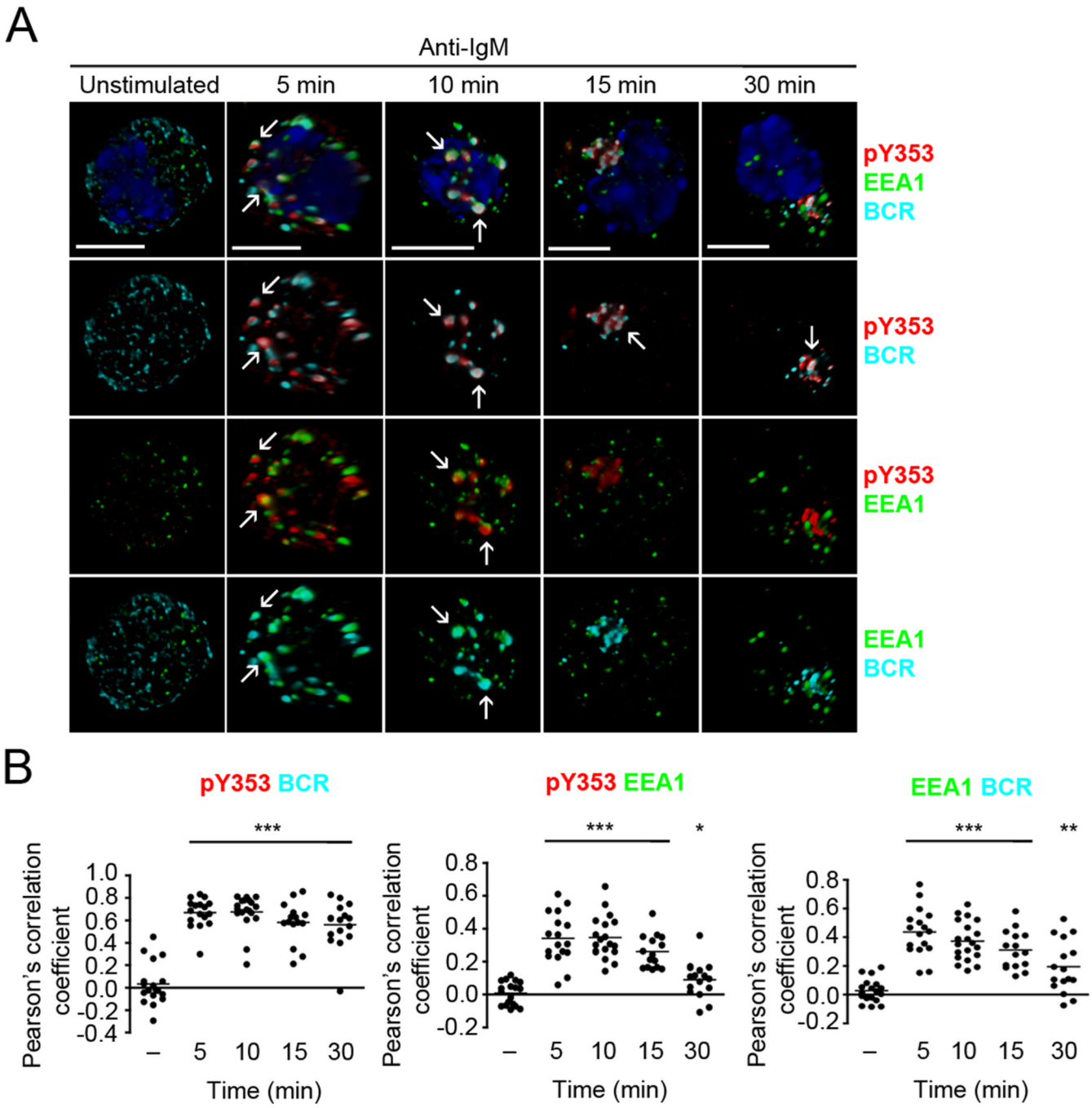

Figure 4. Y353-phosphorylated ezrin co-traffics with the BCR in early endosomes

(A) CH27 B cells were stimulated with 10 μg/ml of anti-IgM for the indicated time and stained for BCR (cyan), pY353 (red), EEA1 (green) and nucleus (blue). Volumetric renditions of representative cells at each time of stimulation are shown, with arrows pointing to overall and pairwise co-localization between Y353-phosphorylated ezrin, BCR and EEA1. Scale bar, 10 μm. **(B)** Pearson's co-localization coefficients for the indicated pairs. Each dot represents an individual cell and horizontal lines indicate the mean (n=15–20 cells per group). Statistical significance is shown for the indicated stimulated groups in comparison to the unstimulated group.

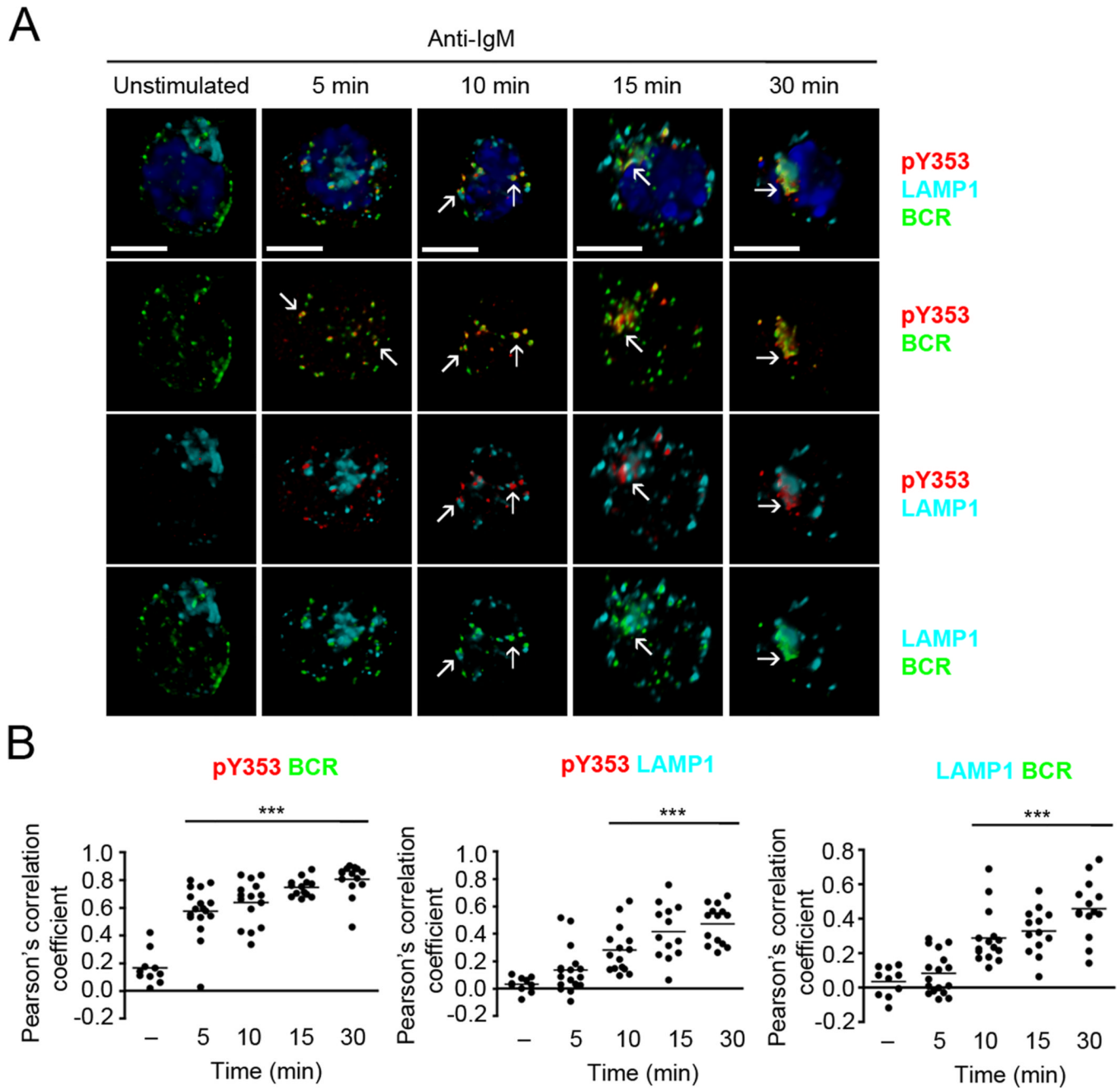

Figure 5. Y353-phosphorylated ezrin and BCR continue to co-localize in late endosomes

(A) CH27 cells were stimulated with 10 μg/ml of anti-IgM for the indicated time and stained for BCR (green), pY353 (red), LAMP1 (cyan) and nucleus (blue). Volumetric renditions of representative cells at each time of stimulation are shown, with arrows pointing to overall and pairwise co-localization between Y353-phosphorylated ezrin, BCR and LAMP1. Scale bar, 10 μm. **(B)** Pearson's co-localization coefficients for the indicated pairs. Each dot represents an individual cell and horizontal lines indicate the mean (n=15–20 cells per group). Statistical significance is shown for the indicated stimulated groups in comparison to the unstimulated group.

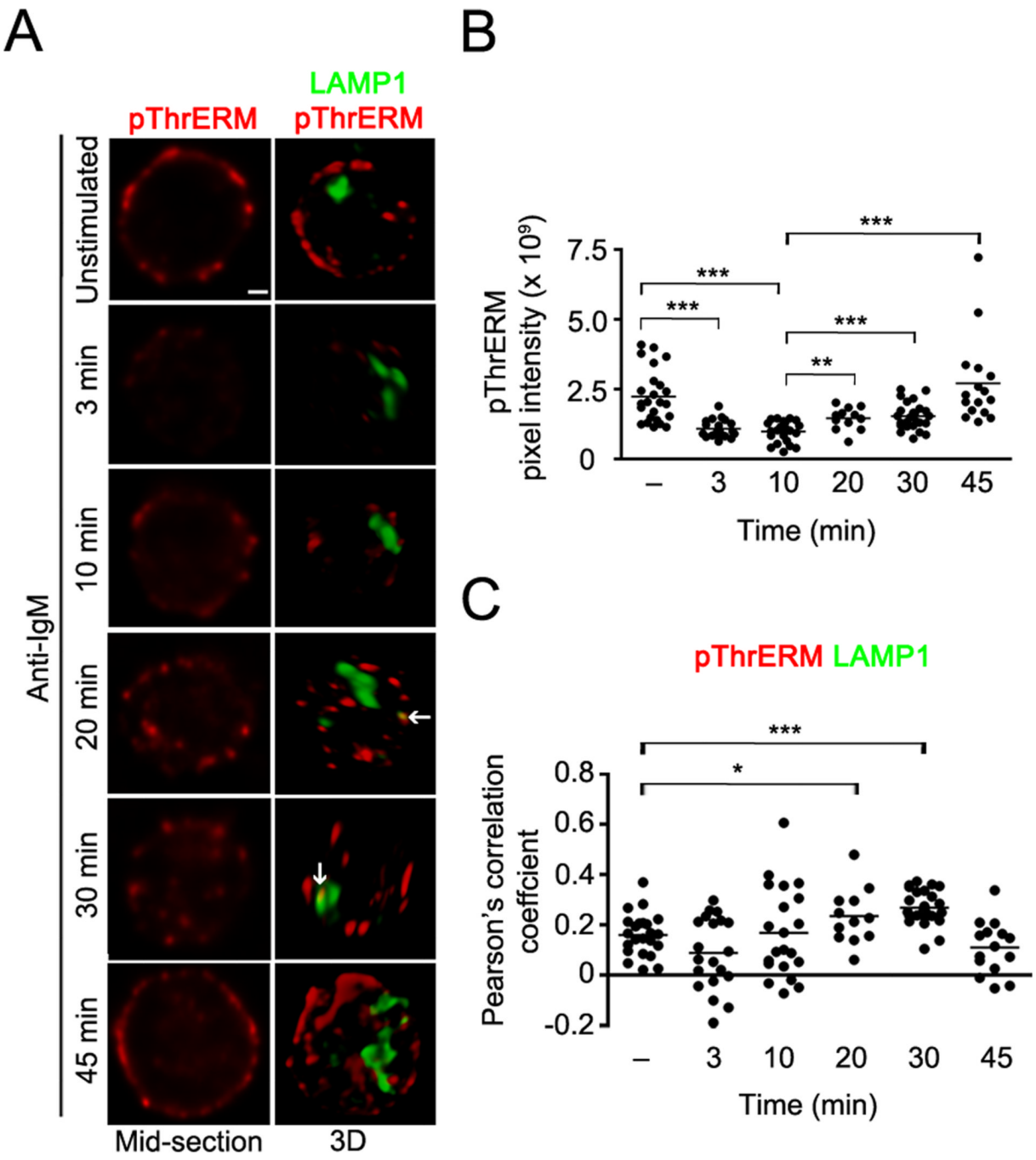

Figure 6. T567 rephosphorylation of ezrin occurs at the plasma membrane and in late endosomes

(A) CH27 cells were stimulated with 10 μg/ml of anti-IgM for the indicated time and stained for pThrERM (red) and LAMP1 (green). Middle plane (left column) and volumetric renditions (right column) of representative cells at each time of stimulation are shown, with arrows pointing to co-localization between pThrERM and LAMP1. Scale bar, 1 μm. Data are representative of two independent experiments. **(B)** Pixel intensity of pThrERM at the plasma membrane. **(C)** Pearson's co-localization coefficients for pThrERM and LAMP1. Each symbol in (B) and (C) represents an individual cell and horizontal lines indicate the mean (n=15–20 cells per group).

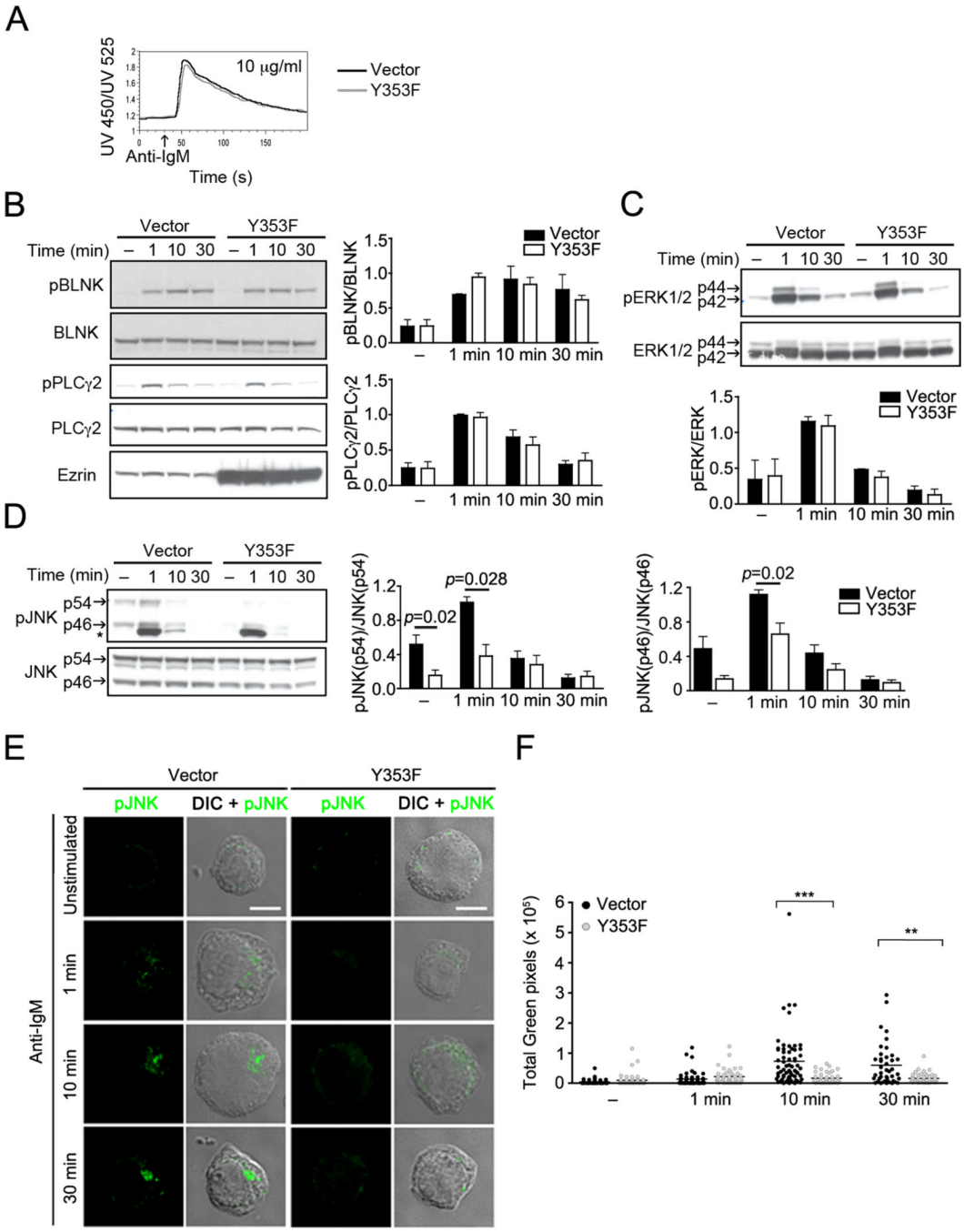

Figure 7. Expression of Y353F mutant of ezrin specifically impairs JNK signaling

(A) CH27 cells transfected with the vector pI2E (Vector) or the Y353F mutant of ezrin (Y353F) were stimulated with 10 μg/ml of anti-IgM and calcium flux measured by ratiometric flow cytometry. Data are representative of three independent experiments. CH27 cells transfected with the vector alone or the Y353F mutant were stimulated with 10 μg/ml of anti-IgM for the indicated time and lysates were probed with **(B)** pBLNK, BLNK, pPLCγ2, PLCγ2, and ezrin or **(C)** pERK and ERK, or **(D)** pJNK and JNK antibodies. Asterix (*) denotes a non-specific protein cross-reacting with the pJNK antibody in lysates from CH27 cells. The bar graphs show ratios of phosphoprotein to the respective total

protein. Data in (B), (C), and (D) are averaged from three independent experiments (mean ±SD). **(E)** CH27 cells transfected with vector or Y353F were stimulated with 10 μg/ml of anti-IgM for the indicated time, stained for pJNK, and a z-stack of images was acquired. Scale bar, 5 μm. Representative cells from each stimulation time are shown. **(F)** Quantification of total green (pJNK) pixels, the horizontal bar indicates the mean (n=42 to 64 cells per group).

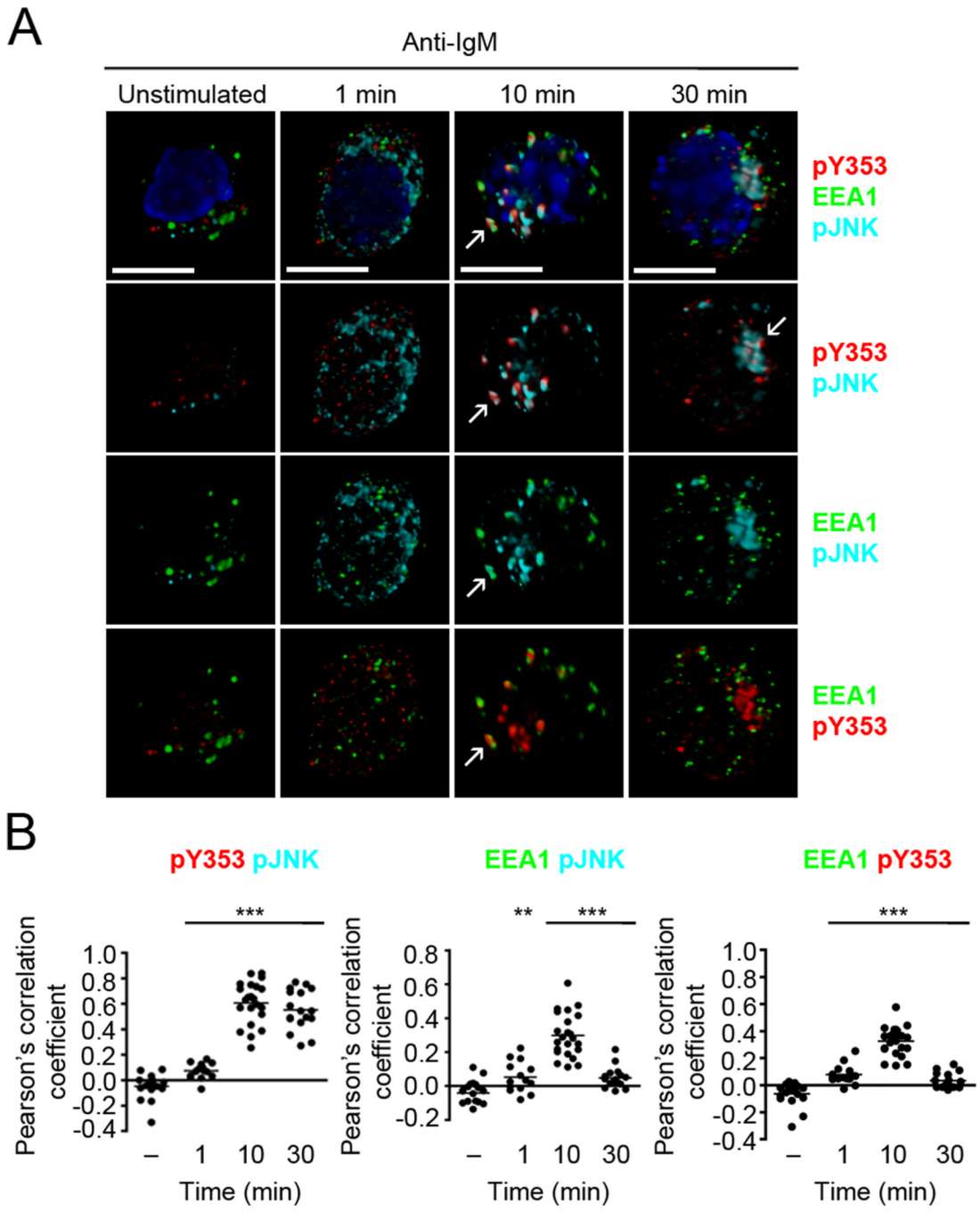

Figure 8. Y353-phosphorylated ezrin co-localizes with active JNK in early endosomes

(A) CH27 B cells were stimulated with 10 μg/ml of anti-IgM for the indicated times and stained for pJNK (cyan), pY353 (red), EEA1 (green) and nucleus (blue). Volumetric renditions of representative cells at each time of stimulation are shown, with arrows pointing to overall and pairwise co-localization between Y353-phosphorylated ezrin, pJNK and EEA1. Scale bar, 10 μm. **(B)** Pearson's co-localization coefficients for the indicated pairs. Each dot represents an individual cell and horizontal lines indicate the mean (n=15–20 per group). Statistical significance is shown for the indicated stimulated groups in comparison to the unstimulated group.

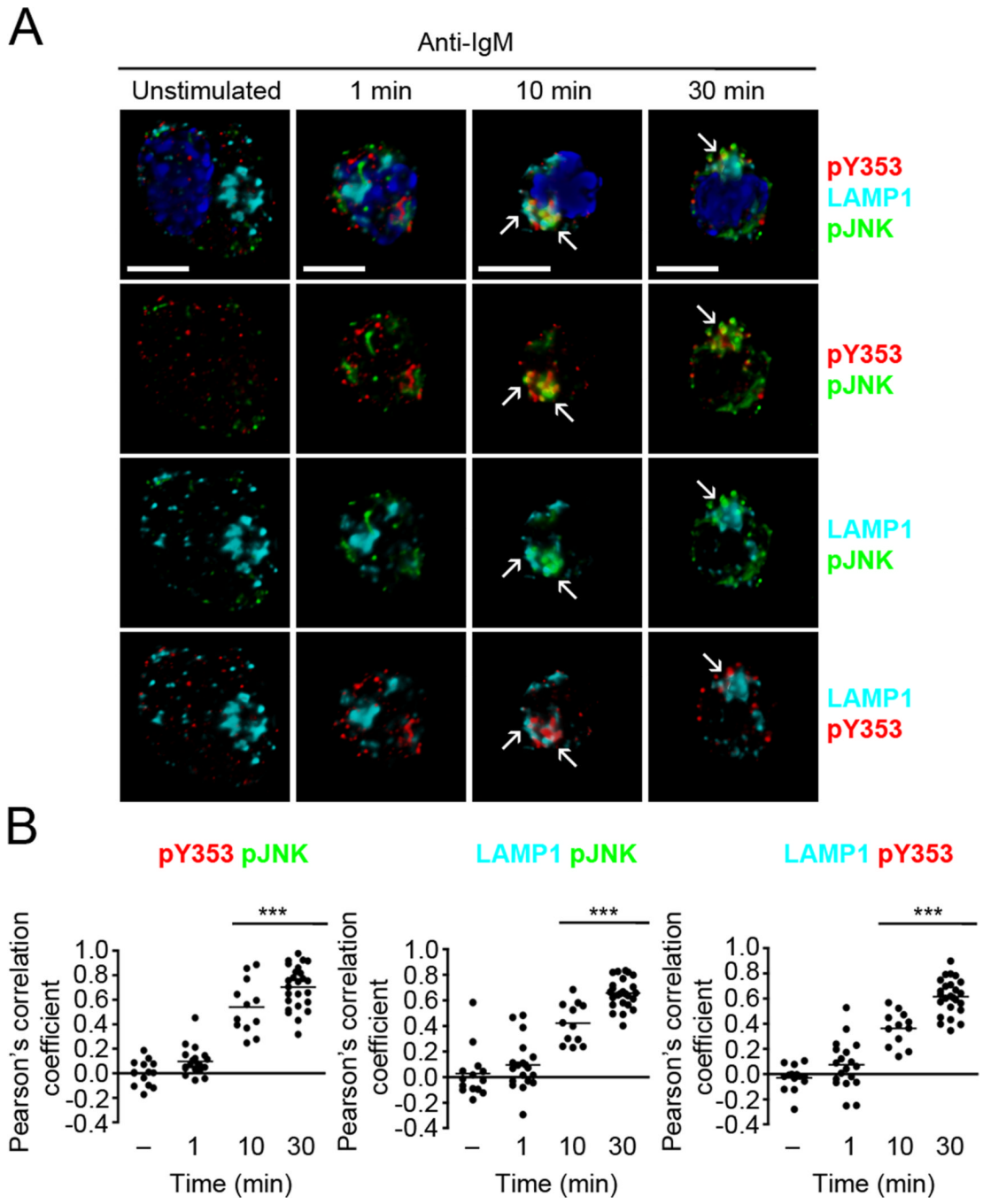

Figure 9. Y353-phosphorylated ezrin and active JNK remain co-localized in late endosomes

(A) CH27 B cells were stimulated with 10 μg/ml of anti-IgM for the indicated times and stained for pJNK (green), pY353 (red), LAMP1 (cyan) and nucleus (blue). Volumetric renditions of representative cells from each time of stimulation are shown, with arrows pointing to overall and pairwise co-localization between Y353-phosphorylated ezrin, pJNK and LAMP1. Scale bar, 10 μm. **(B)** Pearson's co-localization coefficients for the indicated pairs. Each dot represents an individual cell and horizontal lines indicate the mean (n=15–20 per group). Statistical significance is shown for the indicated stimulated groups in comparison to the unstimulated group.

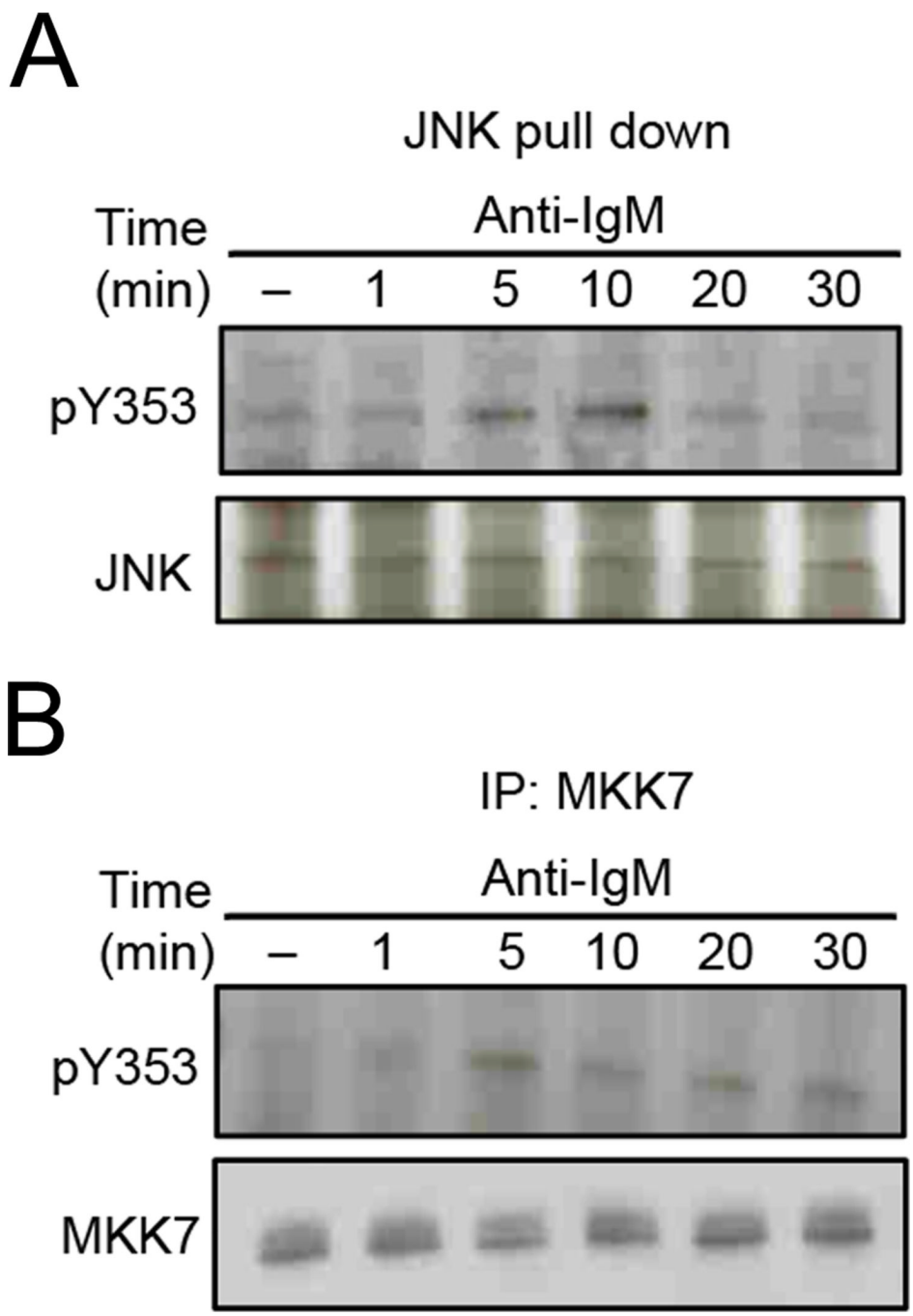

Figure 10. Ezrin physically associates with JNK activation components

CH27 cells were stimulated with 10 μg/ml of anti-IgM for the indicated time, and lysates subjected to precipitation with **(A)** GST-c-Jun fusion protein-Sepharose beads, or **(B)** MKK7 antibody and protein G agarose beads. The precipitates were probed with antibodies to pY353, and (A) JNK or (B) MKK7 antibody. Data in each panel are representative of two independent experiments.

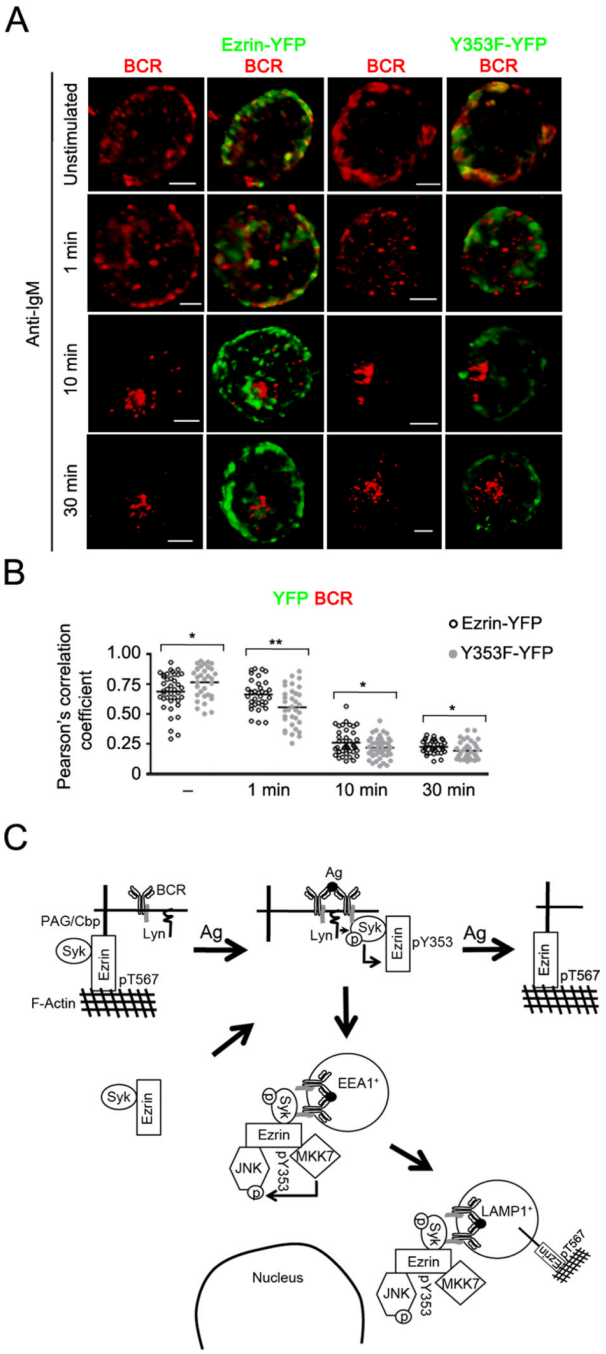

Figure 11. Y353F mutant of ezrin shows reduced co-localization with the internalized BCR

(A) CH27 cells transfected with the Ezrin-YFP or Y353F-YFP fusion constructs of ezrin were stimulated with 10 μg/ml of anti-IgM for the indicated time, stained for BCR, and a z-stack of images was acquired. Volumetric renditions of representative cells from each stimulation time are shown. Scale bar, 5 μm. Data are representative of two independent experiments. **(B)** Pearson's co-localization coefficients for YFP fusion protein and the BCR are shown. Each symbol represents an individual cell and horizontal lines indicate the mean (n=15–20 cells per group). **(C)** The model of endosomal regulation of BCR crosslinking-induced JNK activation by Y353-phosphorylated ezrin. Syk associates constitutively with a

pool of either active, cortical ezrin bound to PAG, or inactive, cytosolic fraction of ezrin. Upon BCR ligation by antigen Lyn-mediated phosphorylation of the BCR ITAMs recruits Syk and Syk-associated ezrin, leading to Syk-dependent phosphorylation of ezrin at Y353. The Y353-phosphorylated ezrin associates with JNK and its kinase MKK7, and localizes them in the vicinity of the internalized BCRs that traffic within the early ($EEA1^+$) followed by late endosomes ($LAMP1^+$). The threonine phosphorylation of ezrin recovers within late endosomes at 30 min and at the plasma membrane between 20 and 45 min of BCR stimulation.